AIMS Mathematics, 9(9): 25732–25751.
DOI: 10.3934/math.20241257
Received: 13 May 2024
Revised: 30 August 2024
Accepted: 02 September 2024
Published: 04 September 2024

http://www.aimspress.com/journal/Math

Research article

New traveling wave solutions, phase portrait and chaotic patterns for the dispersive concatenation model with spatio-temporal dispersion having multiplicative white noise

Da Shi, Zhao Li* and Dan Chen

College of Computer Science, Chengdu University, Chengdu, 610106, China

* **Correspondence:** Email: lizhao10.26@163.com.

Abstract: This article studied the new traveling wave solutions of the cascaded model with higher-order dispersion effects combined with the effects of spatiotemporal dispersion and multiplicative white noise. In the process of exploring traveling wave solutions, a clever combination of the polynomial complete discriminant system was used to discover more forms of traveling wave solutions for this equation. In order to better observe and analyze the propagation characteristics of traveling wave solutions, we used Maple and Matlab software to provide two-dimensional and three-dimensional visualization displays of the equation solutions. Meanwhile, we also analyzed the internal mechanism of nonlinear partial differential equations using planar dynamical systems. The research results indicated that there are differences in the results of different forms of soliton solutions affected by external random factors, which provided more beneficial references for people to better understand the cascaded model with higher-order dispersion effects combined with the effects of spatiotemporal dispersion and multiplicative white noise, and helped people to more comprehensively understand the propagation characteristics of optical solitons. The solution method in this article was also applicable to the study of other nonlinear partial differential equations.

Keywords: dispersive concatenation model; phase portraits; spatio-temporal dispersion; complete discriminant system; multiplicative white noise; traveling wave solutions
Mathematics Subject Classification: 35B20, 35C05, 35C07, 35C09

1. Introduction

The term soliton is an important concept in modern mathematics and physics. From fluid mechanics, plasma, condensed matter physics, elementary particle theory to astrophysics, solitons have been found everywhere. In 1973, Akira and Frederick [1, 2] first proposed the concept of optical soliton and theoretically proved that optical pulses in any lossless fiber can deform into solitons during

transmission and then stably transmit. Subsequently, people successively discovered bright solitons, dark solitons, black solitons, and gray solitons [3, 4]. Due to the fact that optical soliton transmission does not change its waveform and speed, optical soliton communication quickly developed. With the urgent demand for long-distance and high-capacity optical communication, the transmission evolution of soliton pulses in optical fibers is also receiving increasing attention. With the continuous deepening of research on solitons, people have gradually established relatively complete mathematical and physical soliton theories, especially using nonlinear partial differential equations to establish some typical solitary wave equations: the Korteweg-de Vries (KdV) equation, Sine Gordon (SG) equation, and nonlinear Schrödinger (NLS) equation. For the solutions of these equations, researchers applied the modified extended tanh function method [5, 6], traveling wave transformation method [7], Jacobi elliptic function expansion method [8], the improved direct algebraic scheme [9], the sub-equation method [10], Lie symmetry analysis [11, 12], Painlevé analysis [13, 14], Bäcklund transformation method [15], the Darboux transformation method [16], and other methods to actively explore the numerical and exact solutions of solitary wave equations, where they have achieved many results. However, most studies are mainly limited to ideal conditions that ignore the influence of external factors on transmission models. In fact, in actual communication systems, various types of noise cannot be avoided. When studying the transmission law of optical solitons in noisy environments, it is necessary to establish a random optical soliton transmission model. That is to say, when considering the influence of various external disturbances on the transmission model of optical solitons, it is necessary to use a random Schrödinger square to describe its transmission law. In references [17, 18], the author used white noise functional analysis to study multiple Wick type stochastic models and achieved a number of results. However, more research is needed on the exact solution methods for solitary wave equations with random perturbations.

In our study, we contemplated the dimensionless expression of the cascaded model with higher-order dispersion effects, combined with the effects of spatiotemporal dispersion and multiplicative white noise in the Itô sense, which can be described as follows [19]:

$$\begin{aligned} &ip_t + ap_{xx} + bp_{xt} + c|p|^2p - i\tau_1(\beta_1 p_{xxx} + \beta_2|p|^2p_x) + \sigma(p - ibp_x)W_t(t) + \tau_2(\beta_3 p_{xxxx} + \beta_4|p|^2p_{xx} \\ &+ \beta_5|p|^4p + \beta_6|p_x|^2p + \beta_7p_x^2p^* + \beta_8p_{xx}^*p^2) - i\tau_3(\beta_9 p_{xxxxx} + \beta_{10}|p|^2p_{xxx} + \beta_{11}|p|^4p_x + \beta_{12}pp_xp_{xx}^* \\ &+ \beta_{13}p^*p_xp_{xx} + \beta_{14}pp_x^*p_{xx} + \beta_{15}p_x^2p_x^*) = 0. \end{aligned} \tag{1.1}$$

Here, the complex valued function $p = p(x, t)$ stands for the wave profile. Parameter σ is used to reflect the intensity of white noise and is a positive constant, and i is the imaginary unit that satisfies $i^2 = -1$. $W(t)$ is a standard Wiener process which is defined as $W(t) = \int_0^t f(T)dW(T)$, where $T < t$, T stands for a stochastic variable and $W_t(t) = \frac{dW}{dt}$ [20] represents multiplicative white noise. This noise is used to identify the process where the excitation phase is interrupted.

Equation (1.1) investigates the effects of spatiotemporal dispersion and multiplicative white noise on the propagation of optical solitons. Regarding the influence of spatiotemporal dispersion on the propagation of optical solitons, Arnous et al. [19] used an improved Kudryashov method to study the effects of spatiotemporal dispersion and multiplicative white noise on soliton propagation in a cascaded model, and Liu et al. [21] selected an appropriate coefficient function to study the dynamic behavior of single solitons. The authors of Ref. [22] used the improved Kudryashov method to study the effect of spatio-temporal dispersion and multiplicative white noise on the propagation of optical solitons. The authors of Ref. [23] conducted in-depth research on the chaos phenomenon in the cascaded

model and obtained accurate solutions for the cascaded model. Compared with these existing studies, our study provides more forms of accurate solutions and uses planar dynamical systems to perform chaotic analysis on nonlinear systems, enabling people to have a more comprehensive and in-depth understanding of the impact of spatiotemporal dispersion and multiplicative noise on optical soliton propagation in cascaded models, which is conducive to the wider application of optical solitons.

This article includes the following main parts: Section 2 introduces the wave transformation of the solution of Eq (1.1) and proves that the equation has an exact solution with polynomial function modules. Section 3 conducted a planar dynamic system analysis on Eq (1.1). Section 4 provides a detailed derivation process for the exact solution of optical solitons based on the polynomial complete discriminant system classification, obtaining more forms of traveling wave solutions. Section 5 provides visualization analysis of the solutions. Finally, we provide our research conclusion.

2. Mathematical analysis

This article considered the traveling wave solution of Eq (1.1) in the following form:

$$p(x,t) = Q(\zeta)e^{i\phi(x,t)}. \tag{2.1}$$

The wave variable ζ is defined as

$$\zeta = h(x - vt), \tag{2.2}$$

where h and v are nonzero constants. $Q(\zeta)$ is a real-valued function which stands for the amplitude components of the solutions, v represents the speed of the soliton, and the phase component

$$\phi(x,t) = -\kappa x + \omega t + \sigma W(t) - \frac{3}{2}\sigma^2 t + \theta_0. \tag{2.3}$$

Here, κ stands for the frequency of the solitons, ω denotes to the wave number, and θ_0 represents the phase constant.

By inserting Eqs (2.1)–(2.3) into Eq (1.1) [24] and decomposing the real and imaginary parts of the solution, we can obtain the following expressions:

$$\begin{aligned}
&h^2(10\beta_9\kappa^3\tau_3 - 6\beta_3\kappa^2\tau_2 - 3\beta_1\kappa\tau_1 + a - bv)Q'' + h^4(\beta_3\tau_2 - 5\beta_9\kappa\tau_3)Q^{(4)} \\
&+ (\kappa^4(\beta_3\tau_2 - \beta_9\kappa\tau_3) + \beta_1\kappa^3\tau_1 - a\kappa^2 - (b\kappa - 1)(\sigma^2 - \omega))Q + (\beta_5\tau_2 - \beta_{11}\kappa\tau_3)Q^5 \\
&+ (\kappa^2((\beta_{10} + \beta_{12} + \beta_{13} - \beta_{14} - \beta_{15})\kappa\tau_3 - (\beta_4 - \beta_6 + \beta_7 + \beta_8)\tau_2) - \beta_2\kappa\tau_1 + c)Q^3 \\
&+ h^2((\beta_4 + \beta_8)\tau_2 - (3\beta_{10} + \beta_{12} + \beta_{13} - \beta_{14})\kappa\tau_3)Q^2Q'' \\
&+ h^2((2\beta_{12} - 2(\beta_{13} + \beta_{14}) - \beta_{15})\kappa\tau_3 + (\beta_6 + \beta_7)\tau_2)QQ'^2 = 0.
\end{aligned} \tag{2.4}$$

$$\begin{aligned}
&h(-5\beta_9\kappa^4\tau_3 + 4\beta_3\kappa^3\tau_2 + 3\beta_1\kappa^2\tau_1 - 2a\kappa - b\sigma^2 + b\omega + (b\kappa - 1)v)Q' \\
&- \beta_9\tau_3h^5Q^{(5)} - h^3(2\kappa(2\beta_3\tau_2 - 5\beta_9\kappa\tau_3) + \beta_1\tau_1)Q^{(3)} - \beta_{11}h\tau_3Q^4Q' \\
&- \beta_{10}h^3\tau_3Q^2Q^{(3)} - \beta_{15}h^3\tau_3Q'^3 - (\beta_{12} + \beta_{13} + \beta_{14})\tau_3h^3QQ'Q'' \\
&+ h(\kappa((-3\beta_{10} + \beta_{12} - 3\beta_{13} + \beta_{14} + \beta_{15})\kappa\tau_3 + 2(\beta_4 + \beta_7 - \beta_8)\tau_2) + \beta_2\tau_1)Q^2Q' = 0,
\end{aligned} \tag{2.5}$$

with the following parametric restrictions:

$$\beta_9 = \beta_{10} = \beta_{11} = \beta_{15} = 0, \tag{2.6}$$

and

$$\beta_{12} + \beta_{13} + \beta_{14} = 0. \tag{2.7}$$

Equation (2.5) can be simplified to

$$\begin{aligned} &h(4\beta_3\kappa^3\tau_2 + 3\beta_1\kappa^2\tau_1 - 2a\kappa - b\sigma^2 + b\omega + (b\kappa - 1)v)Q' \\ &- h^3(4\kappa\beta_3\tau_2 + \beta_1\tau_1)Q^{(3)} + h(\kappa(-4\beta_{13}\kappa\tau_3 + 2(\beta_4 + \beta_7 - \beta_8)\tau_2) + \beta_2\tau_1)Q^2Q' = 0. \end{aligned} \tag{2.8}$$

Let the coefficients of the variable in the imaginary part of Eq (2.8) be zero. We can obtain the following parameter values:

$$v = -\frac{4\beta_3\kappa^3\tau_2 + 3\beta_1\kappa^2\tau_1 - 2a\kappa - b\sigma^2 + b\omega}{b\kappa - 1}, \tag{2.9}$$

$$\kappa = \frac{(-2\beta_2\beta_3 + \beta_1\beta_4 + \beta_1\beta_7 - \beta_1\beta_8)\tau_2}{2\beta_1\beta_{13}\tau_3}, \tag{2.10}$$

and Eq (1.1) can be reduced to

$$\begin{aligned} &ip_t + ap_{xx} + bp_{xt} + c|p|^2p - i\tau_1(\beta_1 p_{xxx} + \beta_2|p|^2p_x) + \sigma(p - ibp_x)W_t(t) \\ &+ \tau_2(\beta_3 p_{xxxx} + \beta_4|p|^2p_{xx} + \beta_5|p|^4p + \beta_6|p_x|^2p + \beta_7p_x^2p^* + \beta_8p_{xx}^*p^2) \\ &- i\tau_3(\beta_{12}pp_xp_{xx}^* + \beta_{13}p^*p_xp_{xx} + \beta_{14}pp_x^*p_{xx}) = 0, \end{aligned} \tag{2.11}$$

and Eq (2.4) can be reduced to

$$\begin{aligned} &h^4\beta_3\tau_2Q^{(4)} + h^2(\beta_4\tau_2 + \beta_8\tau_2 + 2\beta_{14}\kappa\tau_3)Q^2Q'' + h^2(-6\beta_3\kappa^2\tau_2 - 3\beta_1\kappa\tau_1 + a - bv)Q'' \\ &+ h^2(-4(\beta_{13} + \beta_{14})\kappa\tau_3 + \beta_6\tau_2 + \beta_7\tau_2)QQ'^2 + \beta_5\tau_2Q^5 \\ &+ (-2\kappa^3\beta_{14}\tau_3 - \kappa^2\beta_4\tau_2 + \kappa^2\beta_6\tau_2 - \kappa^2\beta_7\tau_2 - \kappa^2\beta_8\tau_2 - \beta_2\kappa\tau_1 + c)Q^3 \\ &+ (\beta_3\kappa^4\tau_2 + \beta_1\kappa^3\tau_1 - a\kappa^2 - b\kappa\sigma^2 + b\kappa\omega + \sigma^2 - \omega)Q = 0. \end{aligned} \tag{2.12}$$

Equation (2.12) can be further reduced to

$$h^2Q^{(4)}(\zeta) + \eta_6Q(\zeta)^2Q''(\zeta) + \eta_5Q''(\zeta) + \eta_4Q(\zeta)Q'^2(\zeta) + \eta_3Q(\zeta)^5 + \eta_2Q(\zeta)^3 + \eta_1Q(\zeta) = 0, \tag{2.13}$$

with $\eta_1 = (\beta_3\kappa^4\tau_2 + \beta_1\kappa^3\tau_1 - a\kappa^2 - b\kappa\sigma^2 + b\kappa\omega + \sigma^2 - \omega)/(h^2\beta_3\tau_2)$, $\eta_2 = (-2\kappa^3\beta_{14}\tau_3 - \kappa^2\beta_4\tau_2 + \kappa^2\beta_6\tau_2 - \kappa^2\beta_7\tau_2 - \kappa^2\beta_8\tau_2 - \beta_2\kappa\tau_1 + c)/(h^2\beta_3\tau_2)$, $\eta_3 = (\beta_5)/(h^2\beta_3)$, $\eta_4 = (-4(\beta_{13} + \beta_{14})\kappa\tau_3 + \beta_6\tau_2 + \beta_7\tau_2)/(\beta_3\tau_2)$, $\eta_5 = (-6\beta_3\kappa^2\tau_2 - 3\beta_1\kappa\tau_1 + a - bv)/(\beta_3\tau_2)$, $\eta_6 = (\beta_4\tau_2 + \beta_8\tau_2 + 2\beta_{14}\kappa\tau_3)/(\beta_3\tau_2)$, where $h^2\beta_3\tau_2 \neq 0$.

By the trial equation method [25], Eq (2.13) has a polynomial solution $Q(\zeta)$, which satisfies the following equation:

$$Q''(\zeta) = \alpha_0 + \alpha_1Q + \alpha_3Q^3. \tag{2.14}$$

Suppose Eq (2.13) has the following polynomial solution $Q(\zeta)$:

$$Q''(\zeta) = F(Q) = \alpha_0 + \alpha_1Q + \alpha_2Q^2 + \alpha_3Q^3. \tag{2.15}$$

After integrating Eq (2.15), it can be concluded that:

$$(Q')^2 = \frac{1}{2}\alpha_3Q^4 + \frac{2}{3}\alpha_2Q^3 + \alpha_1Q^2 + 2\alpha_0Q + d. \tag{2.16}$$

Taking the derivative of Eq (2.16) yields:

$$Q^{(3)} = \alpha_1 Q' + 2\alpha_2 QQ' + 3\alpha_3 Q^2 Q', \tag{2.17}$$

and from Eq (2.17), we can obtain

$$\begin{aligned} Q^{(4)} = {} & 6\alpha_3^2 Q^5 + 10\alpha_2\alpha_3 Q^4 + (10\alpha_1\alpha_3 + \frac{10}{3}\alpha_2^2)Q^3 \\ & + (5\alpha_1\alpha_2 + 15\alpha_0\alpha_3)Q^2 + (\alpha_1^2 + 6\alpha_0\alpha_2 + 6\alpha_3 d)Q + \alpha_0\alpha_1 + 2\alpha_2 d. \end{aligned} \tag{2.18}$$

Substituting Eqs (2.16)–(2.18) into Eq (2.13), it can be concluded that:

$$\begin{aligned} & (6h^2\alpha_3^2 + \alpha_3\eta_6 + \frac{1}{2}\alpha_3\eta_4 + \eta_3)Q^5 + (10h^2\alpha_2\alpha_3 + \alpha_2\eta_6 + \frac{2}{3}\alpha_2\eta_4)Q^4 \\ & + (10h^2\alpha_1\alpha_3 + \frac{10}{3}h^2\alpha_2^2 + \alpha_1\eta_6 + \alpha_3\eta_5 + \alpha_1\eta_4 + \eta_2)Q^3 \\ & + (5h^2\alpha_1\alpha_2 + 15^2\alpha_0\alpha_3 + \alpha_0\eta_6 + \alpha_2\eta_5 + 2\alpha_0\eta_4)Q^2 \\ & + (h^2\alpha_1^2 + 6h^2\alpha_0\alpha_2 + 6h^2\alpha_3 d + \alpha_1\eta_5 + d\eta_4 + \eta_1)Q + h^2\alpha_0\alpha_1 + 2h^2\alpha_2 d + \alpha_0\eta_5 = 0. \end{aligned} \tag{2.19}$$

Equation (2.19) is a 5th degree equation about the function variable Q. To determine the coefficient $\alpha_i, i = 0, \cdots, 5$, supposing all coefficients of the Eq (2.19) are 0,

$$\begin{cases} 6h^2\alpha_3^2 + \alpha_3\eta_6 + \frac{1}{2}\alpha_3\eta_4 + \eta_3 = 0, \\ 10h^2\alpha_2\alpha_3 + \alpha_2\eta_6 + \frac{2}{3}\alpha_2\eta_4 = 0, \\ 10h^2\alpha_1\alpha_3 + \frac{10}{3}h^2\alpha_2^2 + \alpha_1\eta_6 + \alpha_3\eta_5 + \alpha_1\eta_4 + \eta_2 = 0, \\ 5h^2\alpha_1\alpha_2 + 15h^2\alpha_0\alpha_3 + \alpha_0\eta_6 + \alpha_2\eta_5 + 2\alpha_0\eta_4 = 0, \\ h^2\alpha_1^2 + 6h^2\alpha_0\alpha_2 + 6h^2\alpha_3 d + \alpha_1\eta_5 + d\eta_4 + \eta_1 = 0, \\ h^2\alpha_0\alpha_1 + 2h^2\alpha_2 d + \alpha_0\eta_5 = 0. \end{cases} \tag{2.20}$$

Based on Eq (2.20), we can obtain the following results:

$$\begin{cases} \alpha_3 = \frac{-(2\eta_6+\eta_4) \pm \sqrt{(2\eta_6+\eta_4)^2 - 96h^2\eta_3}}{24h^2}, \ \alpha_2 = 0, \ \alpha_1 = -\frac{\alpha_3\eta_5+\eta_2}{10h^2\alpha_3+\eta_4+\eta_6}, \\ \alpha_0 = 0, \ d = \frac{h^2\alpha_1^2+\alpha_1\eta_5+\eta_1}{6h^2\alpha_3+\eta_4}, \end{cases} \tag{2.21}$$

or

$$\begin{cases} \alpha_3 = \frac{-(2\eta_6+\eta_4) \pm \sqrt{(2\eta_6+\eta_4)^2 - 96h^2\eta_3}}{24h^2}, \ \alpha_2 = 0, \ \alpha_1 = -\frac{\eta_5}{h^2}, \\ \alpha_0 = C, \ d = \frac{h^2\alpha_1^2+\alpha_1\eta_5+\eta_1}{6h^2\alpha_3+\eta_4}, \end{cases} \tag{2.22}$$

where C is an arbitrary nonzero constant.

In either Eq (2.21) or Eq (2.22), the coefficient α_2 is zero, so Eq (2.13) has the solution in the form of Eq (2.14).

3. Phase portraits and chaotic pattern analysis

In order to observe the stability state of the Eq (1.1), as well as the condition of the system being affected by external random factors, we are going to discuss the dynamic behavior [26–29] characteristics of the Eq (1.1).

In the absence of precise expressions for solutions, phase diagram analysis is an effective method for analyzing the behavioral characteristics of solutions.

Equation (2.14) can be expressed as the two-dimensional system of equations in the following form:

$$\begin{cases} \frac{dQ}{d\zeta} = y, \\ \frac{dy}{d\zeta} = \alpha_3 Q^3 + \alpha_1 Q. \end{cases} \tag{3.1}$$

Then, the corresponding Hamilton system of Eq (3.1) is as follows

$$H(Q, y) = \frac{1}{2}y^2 - (\frac{\alpha_1}{2}Q^2 + \frac{\alpha_3}{4}Q^4). \tag{3.2}$$

While $\alpha_1\alpha_3 > 0$, there is an equilibrium point $(0, 0)$ for the system (see Figure 1a,d), and the point $(0, 0)$ is also the saddle point in Figure 1a. While $\alpha_1\alpha_3 < 0$, we can get three equilibrium points of the system: $(0, 0)$, $(-\sqrt{-\frac{\alpha_1}{\alpha_3}}, 0)$, and $(\sqrt{-\frac{\alpha_1}{\alpha_3}}, 0)$ (see Figure 1b,c). From Figure 1b,c,d, we can conclude that Eq (3.1) has periodic solutions because they all comprise closed orbits, while in the case of Figure 1a, Eq (3.1) may contain optical soliton solutions.

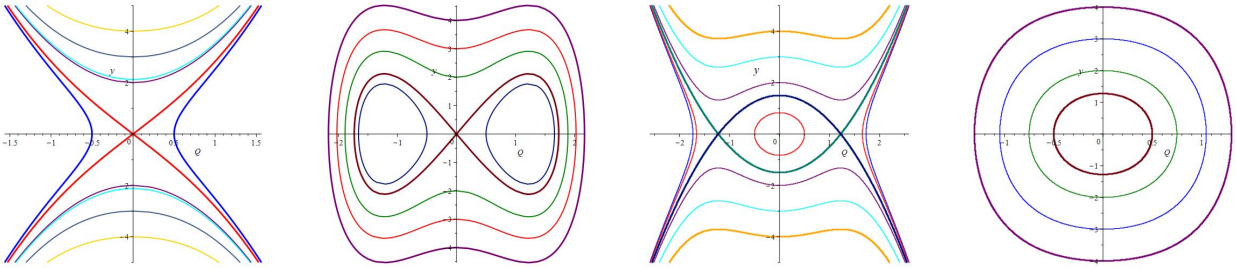

(a) $\alpha_1 < 0, \alpha_3 < 0$ (b) $\alpha_1 < 0, \alpha_3 > 0$ (c) $\alpha_1 > 0, \alpha_3 < 0$ (d) $\alpha_1 > 0, \alpha_3 > 0$

Figure 1. The phase portrait of Eq (3.1).

Next, we add a perturbation factor to Eq (3.1) to to analyze the sensitivity of this system,

$$\begin{cases} \frac{dQ}{d\zeta} = y, \\ \frac{dy}{d\zeta} = \alpha_3 Q^3 + \alpha_1 Q + A\cos(\varpi\zeta), \end{cases} \tag{3.3}$$

where ϖ represents frequency and A represents amplitude.

We fix parameters α_1 and α_3, and adjust the values of A and ϖ to compare the impact of external disturbances on the system. The phase portraits of Figure 2a,b,d,e and the sensitivity analysis of Figure 3 shows that the system is highly sensitive to the influence of frequency, therefore, in practical applications, we should explore appropriate frequencies to ensure stable operation of the system. The

Poincaré sections (see Figure 2c,f) show the existence of chaotic states and quasiperiodic solutions in the system.

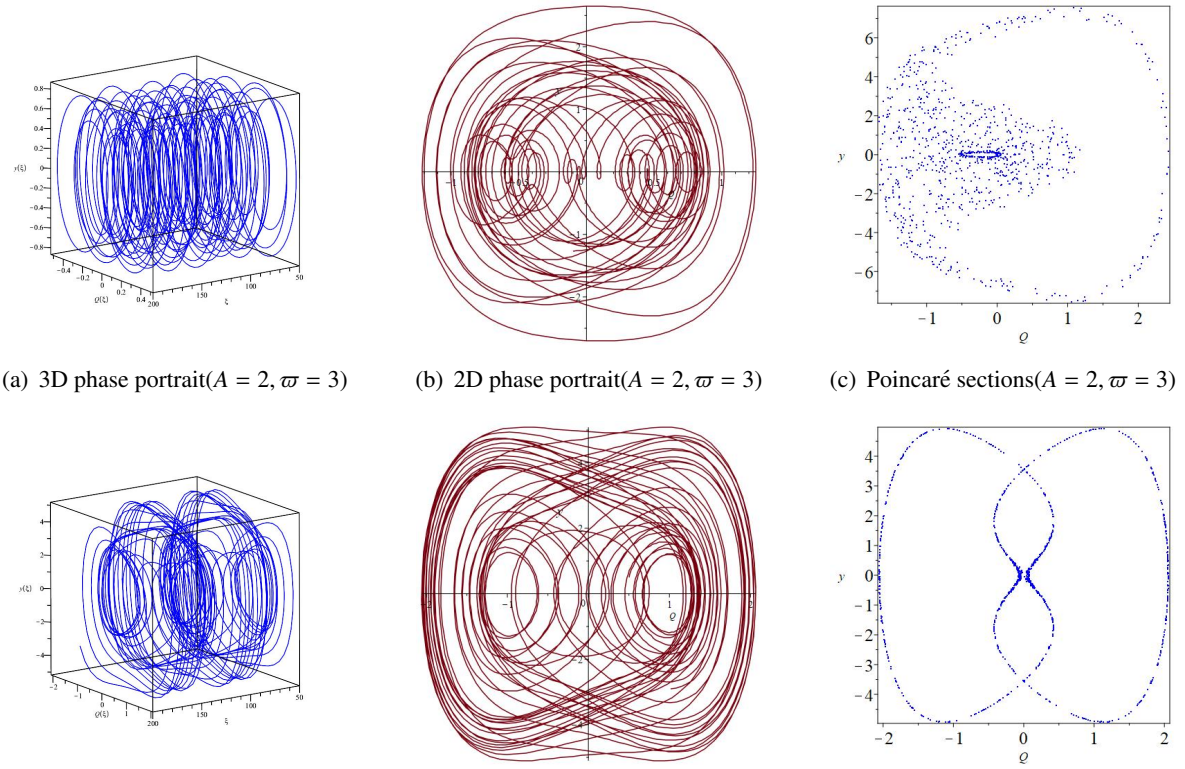

(a) 3D phase portrait($A = 2, \varpi = 3$) (b) 2D phase portrait($A = 2, \varpi = 3$) (c) Poincaré sections($A = 2, \varpi = 3$)

(d) 3D phase portrait($A = 5, \varpi = 1.5$) (e) 2D phase portrait($A = 5, \varpi = 1.5$) (f) Poincaré sections($A = 5, \varpi = 1.5$)

Figure 2. The visualization of the Eq (3.3) with $\alpha_1 = 0.2$, $\alpha_3 = -4$.

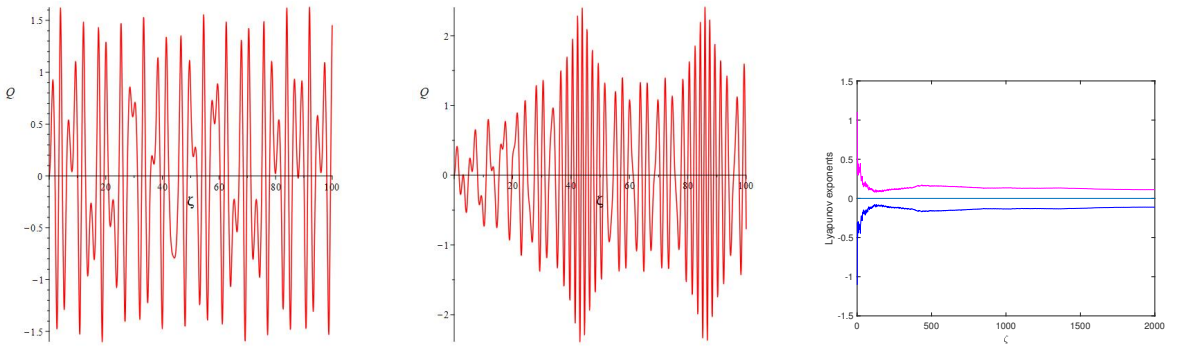

(a) Sensitivity analysis($\varpi = 1.5$) (b) Sensitivity analysis($\varpi = 3$) (c) Lyapunov exponents diagram

Figure 3. Sensitivity analysis of the Eq (3.3) with $\alpha_1 = 0.2$, $\alpha_3 = -4$, $A = 2$.

4. New traveling wave solutions for Eq (1.1)

According to the derivation in Section 2, as long as the solution to Eq (2.16) under Eq (2.21) is obtained, the solution to Eq (2.13) can be obtained.

Assuming

$$\lambda = \frac{2\alpha_1}{\alpha_3}, \ \ \mu = \frac{4\alpha_0}{\alpha_3}, \ \ \tau = \frac{2d}{\alpha_3}, \tag{4.1}$$

then Eq (2.16) can be transformed to

$$\pm\sqrt{\frac{\alpha_3}{2}}(\zeta - \zeta_0) = \int \frac{dQ}{\sqrt{Q^4 + \lambda Q^2 + \mu Q + \tau}} = \int \frac{dQ}{\sqrt{F(Q)}}, \tag{4.2}$$

where ζ_0 is an integral constant and $F(Q) = Q^4 + \lambda Q^2 + \mu Q + \tau$.

According the complete discriminant system for fourth order polynomials [30]

$$\begin{cases} D_1 = 4, \\ D_2 = -\lambda, \\ D_3 = -2\lambda^3 + 8\lambda\tau - 9\mu^2, \\ D_4 = -\lambda^3\mu^2 + 4\lambda^4\tau + 36\lambda\mu^2\tau - 32\lambda^2\tau^2 - \frac{27}{4}\mu^4 + 64\tau^3, \\ E_2 = 9\lambda^2 - 32\lambda\tau, \end{cases} \tag{4.3}$$

the roots of quartic polynomials $F(x) = x^4 + \lambda x^2 + \mu x + \tau$ can be classified into the following types:

(i) If $D_2 < 0$, $D_3 = 0$, $D_4 = 0$, then $F(x)$ has a pair of conjugate complex roots.

(ii) If $D_2 = 0$, $D_3 = 0$, $D_4 = 0$, then $F(x)$ has one quadruple root.

(iii) If $D_2 > 0$, $D_3 = 0$, $D_4 = 0$, $E_2 > 0$, then $F(x)$ has two different double real roots.

(iv) If $D_2 > 0$, $D_3 > 0$, $D_4 = 0$, then $F(x)$ has one double real root and two single real roots.

(v) If $D_2 > 0$, $D_3 = 0$, $D_4 = 0$, $E_2 = 0$, then $F(x)$ has a triple real root and a single real root.

(vi) If $D_2D_3 < 0$, $D_4 = 0$, then $F(x)$ has a double real root and a pair of conjugate complex roots.

(vii) If $D_1 > 0$, $D_3 > 0$, $D_4 > 0$, then $F(x)$ has four real roots.

(viii) If $D_2D_3 \geq 0$, $D_4 < 0$, then $F(x)$ has two different real roots and a pair of conjugate complex roots.

(ix) If $D_2D_3 \leq 0$, $D_4 > 0$, then $F(x)$ has two pair of conjugate complex roots.

According to the Liu's classification for the roots of quartic polynomials (see [30]), we can derive the following solutions of Eq (1.1):

When $D_2 < 0$, $D_3 = 0$, $D_4 = 0$, Eq (1.1) admits the following solution:

$$p_1(x,t) = [s\tan[s\sqrt{\frac{\alpha_3}{2}}(h(x - vt) - \zeta_0)] + l]e^{i(-\kappa x + \omega t + \sigma W(t) - \frac{3}{2}\sigma^2 t + \theta_0)}. \tag{4.4}$$

When $D_2 < 0$, $D_3 = 0$, $D_4 = 0$, $F(Q)$ has a pair of conjugate complex roots, namely: $F(Q) = [(Q - l)^2 + s^2]^2$. Here, l and s are both real numbers, and $s > 0$. So, Eq (4.2) can be transformed into

$$\pm\sqrt{\frac{\alpha_3}{2}}(\zeta - \zeta_0) = \int \frac{dQ}{(Q - l)^2 + s^2} = \frac{1}{s}\arctan\frac{Q - l}{s}. \tag{4.5}$$

So, we can get the solution to Eq (2.16):

$$Q = s\tan[s\sqrt{\frac{\alpha_3}{2}}(\zeta - \zeta_0)] + l. \tag{4.6}$$

Inserting Eq (4.6) into Eq (2.1), the exact solution $p_1(x,t)$ of Eq (1.1) can be attained.
When $D_2 = 0$, $D_3 = 0$, $D_4 = 0$, Eq (1.1) admits the following solution:

$$p_2(x,t) = -\frac{\sqrt{2}}{\sqrt{\alpha_3}(h(x-vt) - \zeta_0)} e^{i(-\kappa x + \omega t + \sigma W(t) - \frac{3}{2}\sigma^2 t + \theta_0)}. \tag{4.7}$$

If $D_2 = 0$, $D_3 = 0$, $D_4 = 0$, $F(Q)$ has one quadruple root, namely: $F(Q) = Q^4$. Then, Eq (4.2) can be transformed into

$$\pm\sqrt{\frac{\alpha_3}{2}}(\zeta - \zeta_0) = \int \frac{dQ}{Q^2} = -Q^{-1}. \tag{4.8}$$

So, the solution to Eq (2.16) can be described as follows

$$Q = -\frac{\sqrt{2}}{\sqrt{\alpha_3}(\zeta - \zeta_0)}. \tag{4.9}$$

Substituting Eq (4.9) into Eq (2.1), the exact solution $p_2(x,t)$ of Eq (1.1) can be attained.
When $D_2 > 0$, $D_3 = 0$, $D_4 = 0$, $E_2 > 0$, the following solutions of Eq (1.1) can be derived:

$$p_3(x,t) = [\frac{l-s}{2}[\coth[\sqrt{\frac{\alpha_3}{8}}(s-l)(h(x-vt) - \zeta_0)] - 1] + l]e^{i(-\kappa x + \omega t + \sigma W(t) - \frac{3}{2}\sigma^2 t + \theta_0)}, \tag{4.10}$$

$$p_4(x,t) = [\frac{l-s}{2}[\tanh[\sqrt{\frac{\alpha_3}{8}}(s-l)(h(x-vt) - \zeta_0)] - 1] + l]e^{i(-\kappa x + \omega t + \sigma W(t) - \frac{3}{2}\sigma^2 t + \theta_0)}. \tag{4.11}$$

If $D_2 > 0$, $D_3 = 0$, $D_4 = 0$, $E_2 > 0$, $F(Q)$ has two different double real roots, namely: $F(Q) = (Q-s)^2(Q-l)^2$. Here, l and s are both real numbers, and $s > l$. From Eq (4.2), we can obtain

$$\pm\sqrt{\frac{\alpha_3}{2}}(\zeta - \zeta_0) = \int \frac{dQ}{(Q-s)(Q-l)} = \frac{1}{s-l}\ln|\frac{Q-s}{Q-l}|. \tag{4.12}$$

When $Q > s$ or $Q < l$, the solution to Eq (2.16) can be derived:

$$Q = -\frac{l-s}{e^{\sqrt{\frac{\alpha_3}{2}}(s-l)(\zeta-\zeta_0)} - 1} + l = \frac{l-s}{2}[\coth[\sqrt{\frac{\alpha_3}{8}}(s-l)(\zeta - \zeta_0)] - 1] + l. \tag{4.13}$$

When $l < Q < s$, the solution to Eq (2.16) can be derived:

$$Q = -\frac{l-s}{-e^{\sqrt{\frac{\alpha_3}{2}}(s-l)(\zeta-\zeta_0)} - 1} + l = \frac{l-s}{2}[\tanh[\sqrt{\frac{\alpha_3}{8}}(s-l)(\zeta - \zeta_0)] - 1] + l. \tag{4.14}$$

Uniting Eq (4.9) and Eq (2.1), we can get the exact solutions $p_3(x,t)$ and $p_4(x,t)$ of Eq (1.1).
When $D_2 > 0$, $D_3 > 0$, $D_4 = 0$, Eq (1.1) has implicit function solutions.

If $D_2 > 0$, $D_3 > 0$, $D_4 = 0$, $F(Q)$ has one double real root and two single real roots, namely: $F(Q) = (Q-s)^2(Q-l)(Q-m)$. Here, l, s, and m are real numbers, and $l > m$.

When $s > l$ and $Q > l$, from Eq (4.2), we can obtain the implicit function solution of Eq (2.16):

$$\pm\sqrt{\frac{\alpha_3}{2}}(\zeta-\zeta_0) = \frac{1}{(s-l)(s-m)}\ln\frac{[\sqrt{(Q-l)(s-m)}-\sqrt{(s-l)(Q-m)}]^2}{|Q-s|}. \tag{4.15}$$

When $s > l$ and $Q < m$, or $s < m$ and $Q < l$, from Eq (4.2), we can obtain the implicit function solution of Eq (2.16):

$$\pm\sqrt{\frac{\alpha_3}{2}}(\zeta-\zeta_0) = \frac{1}{(s-l)(m-s)}\ln\frac{[\sqrt{(Q-l)(m-s)}-\sqrt{(l-s)(Q-m)}]^2}{|Q-s|}. \tag{4.16}$$

When $l > s > m$ from Eq (4.2), we can obtain the implicit function solution of Eq (2.16):

$$\pm\sqrt{\frac{\alpha_3}{2}}(\zeta-\zeta_0) = \frac{1}{(l-s)(s-m)}\arcsin\frac{(Q-l)(s-m)+(s-l)(Q-m)}{|(Q-s)(l-m)|}. \tag{4.17}$$

By combining Eqs (4.15)–(4.17) and Eq (2.1), the implicit function solution of Eq (1.1) can be acquired.

When $D_2 > 0$, $D_3 = 0$, $D_4 = 0$, $E_2 = 0$, we are able to derive the following solution for Eq (1.1):

$$p_5(x,t) = [\frac{8(s-l)}{\alpha_3(l-s)^2(h(x-vt)-\zeta_0)^2-8}+s]e^{i(-\kappa x+\omega t+\sigma W(t)-\frac{3}{2}\sigma^2 t+\theta_0)}. \tag{4.18}$$

When $D_2 > 0$, $D_3 = 0$, $D_4 = 0$, $E_2 = 0$, $F(Q)$ has a triple real root and a single real root, namely: $F(Q) = (Q-s)^3(Q-l)$. Here, s and l are both real numbers.

When $Q > s$ and $Q > l$, or $Q < s$ and $Q < l$, from Eq (4.2), we can get the solution of Eq (2.16):

$$Q = \frac{8(s-l)}{\alpha_3(l-s)^2(\zeta-\zeta_0)^2-8}+s. \tag{4.19}$$

Accordingly, by combining Eq (4.19) and Eq (2.1), we can derive the exact solution $p_5(x,t)$ of Eq (1.1).

When $D_2D_3 < 0$, $D_4 = 0$, Eq (1.1) has the solution

$$p_6(x,t) = \frac{e^{\pm\sqrt{(s-l)^2+m^2}\sqrt{\frac{\alpha_3}{2}}(h(x-vt)-\zeta_0)}-\gamma+\sqrt{(s-l)^2+m^2}(2-\gamma)}{[e^{\pm\sqrt{(s-l)^2+m^2}\sqrt{\frac{\alpha_3}{2}}(h(x-vt)-\zeta_0)}-\gamma]^2-1}e^{i(-\kappa x+\omega t+\sigma W(t)-\frac{3}{2}\sigma^2 t+\theta_0)}. \tag{4.20}$$

While $D_2D_3 < 0$, $D_4 = 0$, $F(Q)$ has a double real root and a pair of conjugate complex roots, namely: $F(Q) = (Q-s)^2[(Q-l)^2+m^2]$. Here, s, l, and m are real numbers.

Thus, the equivalent form of Eq (4.2) is

$$\pm\sqrt{\frac{\alpha_3}{2}}(\zeta-\zeta_0) = \int\frac{dQ}{(Q-s)\sqrt{(Q-l)^2+m^2}} = \frac{1}{\sqrt{(s-l)^2+m^2}}\ln|\frac{\gamma Q+\delta-\sqrt{(Q-l)^2+m^2}}{Q-s}|, \tag{4.21}$$

where $\gamma = \frac{s-2l}{\sqrt{(s-l)^2+m^2}}$, $\delta = \sqrt{(s-l)^2+m^2}-\frac{s(s-2l)}{\sqrt{(s-l)^2+m^2}}$.

With further derivation, the solution to Eq (2.16) can be described as

$$Q = \frac{e^{\pm\sqrt{(s-l)^2+m^2}\sqrt{\frac{\alpha_3}{2}}(\zeta-\zeta_0)} - \gamma + \sqrt{(s-l)^2+m^2}(2-\gamma)}{[e^{\pm\sqrt{(s-l)^2+m^2}\sqrt{\frac{\alpha_3}{2}}(\zeta-\zeta_0)} - \gamma]^2 - 1}. \tag{4.22}$$

Putting Eq (4.22) into Eq (2.1), the exact solution $p_6(x,t)$ of Eq (1.1) can be derived.

When $D_1 > 0$, $D_3 > 0$, $D_4 > 0$, Eq (1.1) has the solutions

$$p_7(x,t) = \frac{l(s-n)\mathbf{sn}^2(\frac{\sqrt{\alpha_3(s-m)(l-n)}}{2\sqrt{2}}(h(x-vt)-\zeta_0),r) - s(l-n)}{(s-n)\mathbf{sn}^2(\frac{\sqrt{\alpha_3(s-m)(l-n)}}{2\sqrt{2}}(h(x-vt)-\zeta_0),r) - l + n} e^{i(-\kappa x+\omega t+\sigma W(t)-\frac{3}{2}\sigma^2 t+\theta_0)}. \tag{4.23}$$

$$p_8(x,t) = \frac{n(l-m)\mathbf{sn}^2(\frac{\sqrt{\alpha_3(s-m)(l-n)}}{2\sqrt{2}}(h(x-vt)-\zeta_0),r) - m(l-n)}{(l-m)\mathbf{sn}^2(\frac{\sqrt{\alpha_3(s-m)(l-n)}}{2\sqrt{2}}(h(x-vt)-\zeta_0),r) - l + n} e^{i(-\kappa x+\omega t+\sigma W(t)-\frac{3}{2}\sigma^2 t+\theta_0)}. \tag{4.24}$$

While $D_1 > 0$, $D_3 > 0$, $D_4 > 0$, $F(Q)$ has four real roots, namely: $F(Q) = (Q-s)(Q-l)(Q-m)(Q-n)$. Here, s, l, m, and n are real numbers, and $s > l > m > n$.

When $Q > s$ or $Q < n$, the following changes:

$$Q = \frac{l(s-n)\sin^2\varphi - s(l-n)}{(s-n)\sin^2\varphi - (l-n)}. \tag{4.25}$$

When $m < Q < l$, the following changes:

$$Q = \frac{n(l-m)\sin^2\varphi - m(l-n)}{(l-m)\sin^2\varphi - (l-n)}. \tag{4.26}$$

Under the given conditions, Eq (4.2) can be transformed into

$$\sqrt{\frac{\alpha_3}{2}}(\zeta-\zeta_0) = \int \frac{dQ}{\sqrt{(Q-s)(Q-l)(Q-m)(Q-n)}} = \frac{2}{\sqrt{(s-m)(l-n)}} \int \frac{dQ}{\sqrt{1-r^2\sin^2\varphi}}, \tag{4.27}$$

where $r^2 = \frac{(s-n)(l-m)}{(s-m)(l-n)}$.

According to Eq (4.27) and the definition of the Jacobian elliptic sine function, the following conclusions can be obtained:

$$\mathbf{sn}(\frac{\sqrt{\alpha_3(s-m)(l-n)}}{2\sqrt{2}}(\zeta-\zeta_0),r) = \sin\varphi. \tag{4.28}$$

So the corresponding solution of Eq (2.16) is

$$Q = \frac{l(s-n)\mathbf{sn}^2(\frac{\sqrt{\alpha_3(s-m)(l-n)}}{2\sqrt{2}}(\zeta-\zeta_0),r) - s(l-n)}{(s-n)\mathbf{sn}^2(\frac{\sqrt{\alpha_3(s-m)(l-n)}}{2\sqrt{2}}(\zeta-\zeta_0),r) - l + n}, \tag{4.29}$$

and

$$Q = \frac{n(l-m)\mathbf{sn}^2(\frac{\sqrt{\alpha_3(s-m)(l-n)}}{2\sqrt{2}}(\zeta-\zeta_0), r) - m(l-n)}{(l-m)\mathbf{sn}^2(\frac{\sqrt{\alpha_3(s-m)(l-n)}}{2\sqrt{2}}(\zeta-\zeta_0), r) - l + n}, \tag{4.30}$$

Substituting Eqs (4.29) and (4.30) into Eq (2.1), respectively, we can get the exact solutions $p_7(x,t)$ and $p_8(x,t)$ of Eq (1.1).

When $D_2D_3 \geq 0$, $D_4 < 0$, Eq (1.1) has the solution

$$p_9(x,t) = \frac{c_1\mathbf{cn}(\frac{\sqrt{\mp\alpha_3 ne(s-l)}}{2re}(h(x-vt)-\zeta_0), r) + c_2}{c_3\mathbf{cn}(\frac{\sqrt{\mp\alpha_3 ne(s-l)}}{2re}(h(x-vt)-\zeta_0), r) + c_4} e^{i(-\kappa x+\omega t+\sigma W(t)-\frac{3}{2}\sigma^2 t+\theta_0)}. \tag{4.31}$$

If $D_2D_3 \geq 0$, $D_4 < 0$, $F(Q)$ has two different real roots and a pair of conjugate complex roots, namely: $F(Q) = (Q-s)(Q-l)[(Q-m)^2+n^2]$. Here, s, l, m, and n are both real numbers, $s > l$, and $n > 0$.

Introducing the following transformation:

$$Q = \frac{c_1\cos\varphi + c_2}{c_3\cos\varphi + c_4}, \tag{4.32}$$

where $c_1 = \frac{1}{2}(s+l)c_3 - \frac{1}{2}(s-l)c_4$, $c_2 = \frac{1}{2}(s+l)c_4 - \frac{1}{2}(s-l)c_3$, $c_3 = s-m-\frac{n}{e}$, $c_4 = s-m-ne$, $E = \frac{n^2+(s-m)(l-m)}{n(s-l)}$, $e = E - \sqrt{E^2+1}$.

Under the given conditions, Eq (4.2) can be transformed to

$$\sqrt{\frac{\alpha_3}{2}}(\zeta-\zeta_0) = \int \frac{dQ}{\sqrt{\pm(Q-s)(Q-l)[(Q-m)^2+n^2]}} = \frac{2re}{\sqrt{\mp 2ne(s-l)}}\int \frac{dQ}{\sqrt{1-r^2\sin^2\varphi}}, \tag{4.33}$$

where $r^2 = \frac{1}{1+e^2}$.

According to Eq (4.33) and the definition of the Jacobian elliptic cosine function, we can get

$$\mathbf{cn}(\frac{\sqrt{\mp\alpha_3 ne(s-l)}}{2re}(\zeta-\zeta_0), r) = \cos\varphi. \tag{4.34}$$

So the corresponding solution of Eq (2.16) can be depicted as

$$Q = \frac{c_1\mathbf{cn}(\frac{\sqrt{\mp\alpha_3 ne(s-l)}}{2re}(\zeta-\zeta_0), r) + c_2}{c_3\mathbf{cn}(\frac{\sqrt{\mp\alpha_3 ne(s-l)}}{2re}(\zeta-\zeta_0), r) + c_4}, \tag{4.35}$$

and then the exact solution $p_9(x,t)$ of Eq (1.1) can be derived.

When $D_2D_3 \leq 0$, $D_4 > 0$, Eq (1.1) has the solution

$$p_{10}(x,t) = \frac{c_1\mathbf{sn}(\varepsilon(h(x-vt)-\zeta_0), r) + c_2\mathbf{cn}(\varepsilon(h(x-vt)-\zeta_0), r)}{c_3\mathbf{sn}(\varepsilon(h(x-vt)-\zeta_0), r) + c_4\mathbf{cn}(\varepsilon(h(x-vt)-\zeta_0), r)} e^{i(-\kappa x+\omega t+\sigma W(t)-\frac{3}{2}\sigma^2 t+\theta_0)}. \tag{4.36}$$

While $D_2D_3 \leq 0$, $D_4 > 0$, $F(Q)$ has two pairs of conjugate complex roots, namely: $F(Q) = [(Q-s)^2+l^2][(Q-m)^2+n^2]$. Here, s, l, m, and n are real numbers, and $l \geq n > 0$.

Making the following transformation:

$$Q = \frac{c_1 \tan\varphi + c_2}{c_3 \tan\varphi + c_4}, \tag{4.37}$$

where $c_1 = sc_3 + lc_4$, $c_2 = sc_4 - lc_3$, $c_3 = -l - m - \frac{n}{e}$, $c_4 = s - m$, $E = \frac{(s-m)^2+l^2+n^2}{2ln}$, $e = E + \sqrt{E^2 - 1}$.

So, we can obtain the equivalent form of Eq (4.2)

$$\sqrt{\frac{\alpha_3}{2}}(\zeta - \zeta_0) = \int \frac{dQ}{\sqrt{[(Q-s)^2 + l^2][(Q-m)^2 + n^2]}} = \frac{c_3^2 + c_4^2}{n\sqrt{(c_3^2 + c_4^2)(e^2c_3^2 + c_4^2)}} \int \frac{dQ}{\sqrt{1 - r^2\sin^2\varphi}}, \tag{4.38}$$

where $r^2 = \frac{e^2-1}{e^2}$.

According to Eq (4.38) and the definition of the Jacobian elliptic cosine function and the Jacobian elliptic cosine function, we can derive the following results:

$$\mathbf{sn}\left(\frac{n\sqrt{\alpha_3(c_3^2 + c_4^2)(e^2c_3^2 + c_4^2)}}{\sqrt{2}(c_3^2 + c_4^2)}(\zeta - \zeta_0), r\right) = \sin\varphi. \tag{4.39}$$

$$\mathbf{cn}\left(\frac{n\sqrt{\alpha_3(c_3^2 + c_4^2)(e^2c_3^2 + c_4^2)}}{\sqrt{2}(c_3^2 + c_4^2)}(\zeta - \zeta_0), r\right) = \cos\varphi. \tag{4.40}$$

Then we can obtain the solution of Eq (2.16) as

$$Q = \frac{c_1\mathbf{sn}(\varepsilon(\zeta - \zeta_0), r) + c_2\mathbf{cn}(\varepsilon(\zeta - \zeta_0), r)}{c_3\mathbf{sn}(\varepsilon(\zeta - \zeta_0), r) + c_4\mathbf{cn}(\varepsilon(\zeta - \zeta_0), r)}, \tag{4.41}$$

where $\varepsilon = \frac{n\sqrt{\alpha_3(c_3^2+c_4^2)(e^2c_3^2+c_4^2)}}{\sqrt{2}(c_3^2+c_4^2)}$, and the exact solution $p_{10}(x,t)$ of Eq (1.1) can be derived.

5. Graphical representation and discussion

In order to better observe the propagation characteristics of the traveling wave solution of Eq (1.1), we visualized the obtained traveling wave solutions $p_1, p_5, p_7, p_9, p_{10}$ in 2D and 3D graphs with Maple and Matlab software. Figures 4–8 show that traveling wave solitons have distinct shapes and propagation characteristics, specifically, their modulus exhibit different periodic characteristics and prominent changes. The real and imaginary part images of these solutions help people understand the different phases or polarization states of waves, while the modulus images of the solutions can help people understand the amplitude distribution of waves, which plays an important role in understanding phenomena such as wave propagation, reflection, and interference. Figure 4 shows the morphological characteristics of traveling wave solution with tangent function modulus in 2D and 3D graphs. We compare the morphological characteristics of the real and imaginary parts of p_5, p_7, p_9, p_{10} under different intensities of random interference in Figures 5–8. For the traveling wave solution with rational function modulus, its real and imaginary parts undergo significant irregular abrupt changes under low intensity random interference, and its modulus does not exhibit periodic morphological

characteristics (Figure 5). However, Figures 6 and 7 show that the real and imaginary parts of the traveling wave solutions with Jacobian sine function modulus or Jacobian cosine function modulus undergo significant irregular sudden changes under high intensity random interference, and their modulus exhibit periodic morphological characteristics. From Figure 9, we can observe that the traveling wave maintains a certain periodic fluctuation during propagation, but with the enhancement of external random interference, the local mutation of the traveling wave becomes more pronounced.

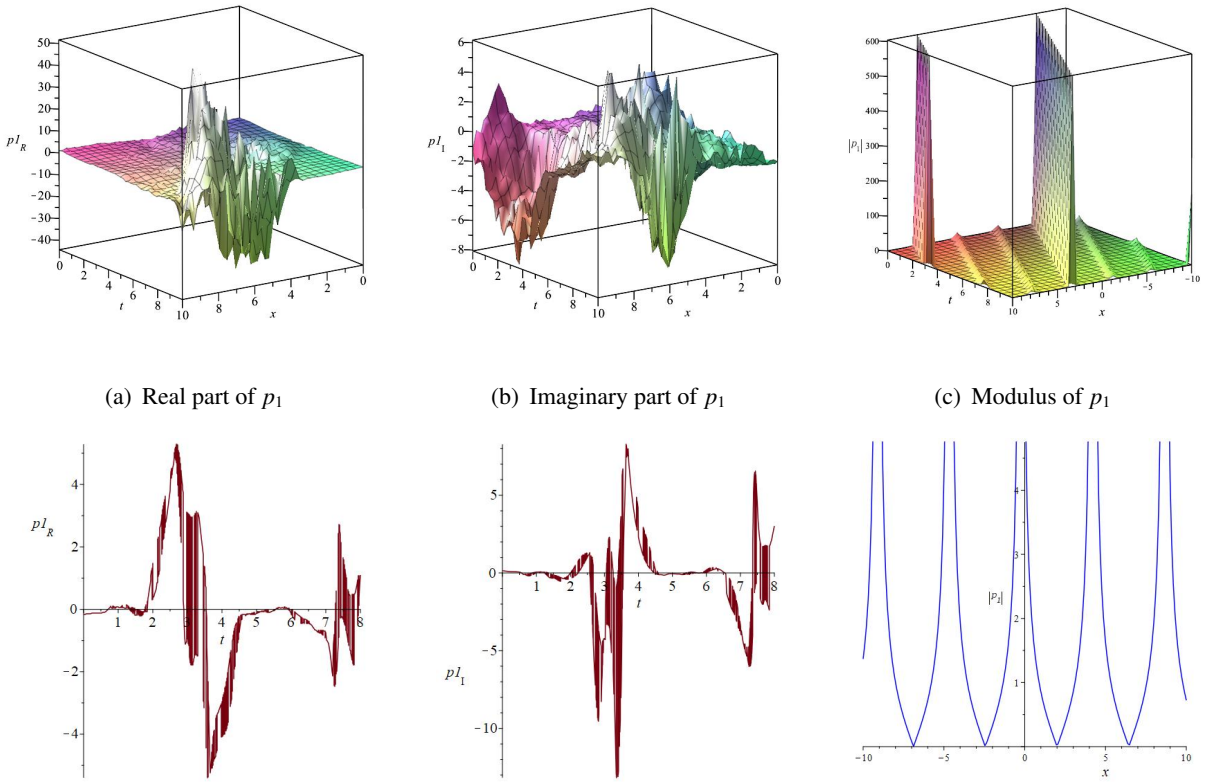

(a) Real part of p_1 (b) Imaginary part of p_1 (c) Modulus of p_1

(d) Real part of p_1 with $x = 1$ (e) Imaginary part of p_1 with $x = 1$ (f) Modulus of p_1 with $x = 1$

Figure 4. The solution p_1 of Eq (1.1) with $\eta_1 = 1$, $\eta_2 = 10.5$, $\eta_3 = 9.5$, $\eta_4 = 1$, $\eta_5 = -5.5$, $\eta_6 = -16$, $\zeta_0 = 0$, and $\sigma = 1$.

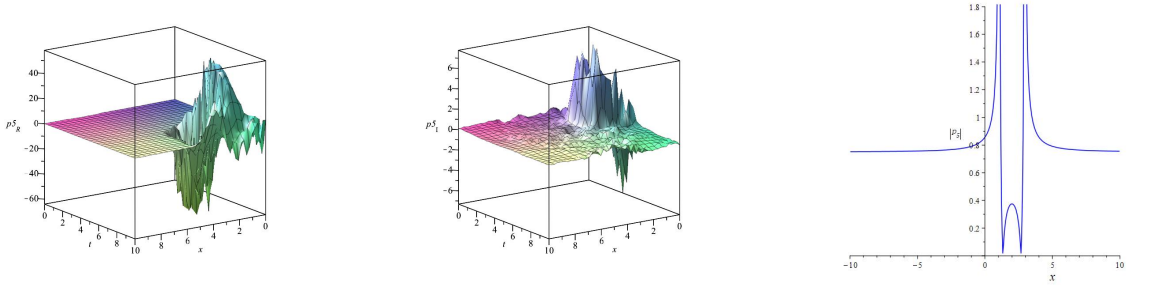

(a) Real part of p_5 with $\sigma = 1$ (b) Imaginary part of p_5 with $\sigma = 1$ (c) Modulus of p_5 with $\sigma = 1, t = 1$

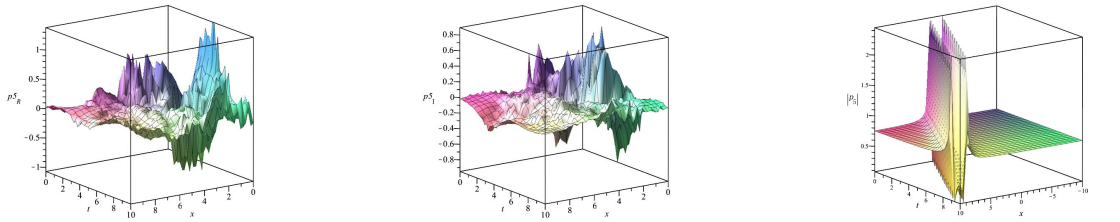

(d) Real part of p_5 with $\sigma = 2$ (e) Imaginary part of p_5 with $\sigma = 2$ (f) Modulus of p_5 with $\sigma = 1$

Figure 5. The solution p_5 of Eq (1.1) with $\eta_1 = 3.322266$, $\eta_2 = -11.8125$, $\eta_3 = 10.5$, $\eta_4 = 1$, $\eta_5 = 1.6875$, $\eta_6 = -17$ and $\zeta_0 = 0$.

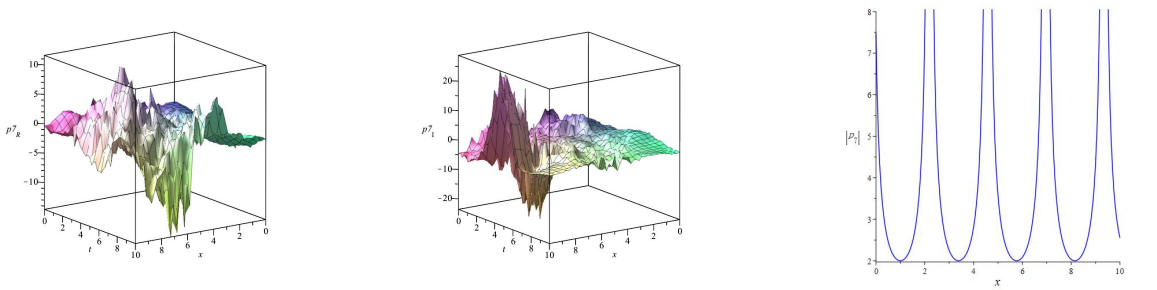

(a) Real part of p_7 with $\sigma = 1$ (b) Imaginary part of p_7 with $\sigma = 1$ (c) Modulus of p_7 with $\sigma = 1, t = 1$

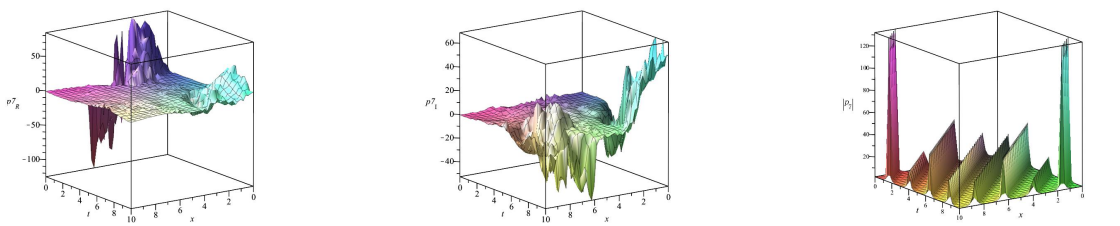

(d) Real part of p_7 with $\sigma = 2$ (e) Imaginary part of p_7 with $\sigma = 2$ (f) Modulus of p_7 with $\sigma = 1$

Figure 6. The solution p_7 of Eq (1.1) with $\eta_1 = 1$, $\eta_2 = -21$, $\eta_3 = 9.5$, $\eta_4 = 1$, $\eta_5 = 8.5$, $\eta_6 = -16$ and $\zeta_0 = 0$.

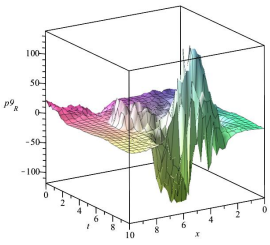

(a) Real part of p_9 with $\sigma = 1$

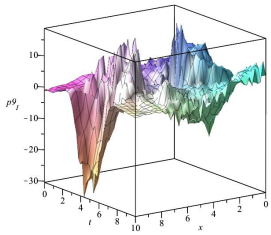

(b) Imaginary part of p_9 with $\sigma = 1$

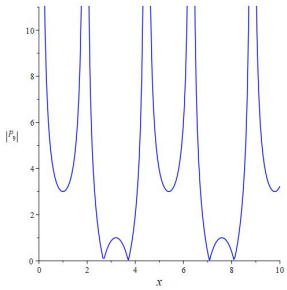

(c) Modulus of p_9 with $\sigma = 1, t = 1$

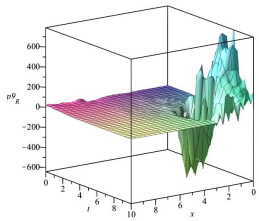

(d) Real part of p_9 with $\sigma = 2$

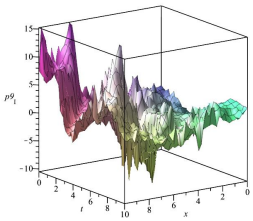

(e) Imaginary part of p_9 with $\sigma = 2$

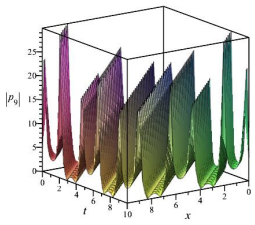

(f) Modulus of p_9 with $\sigma = 1$

Figure 7. The solution p_9 of Eq (1.1) with $\eta_1 = -210$, $\eta_2 = -24.5$, $\eta_3 = 10.5$, $\eta_4 = 1$, $\eta_5 = -3.5$, $\eta_6 = -17$ and $\zeta_0 = 0$.

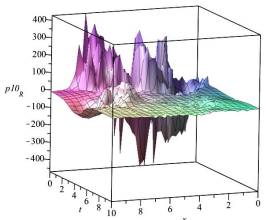

(a) Real part of p_{10} with $\sigma = 1$

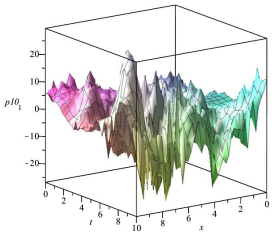

(b) Imaginary part of p_{10} with $\sigma = 1$

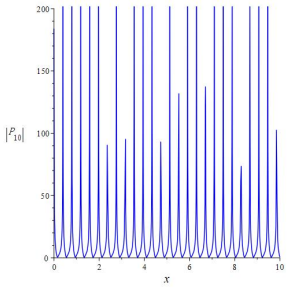

(c) Modulus of p_{10} with $\sigma = 1, t = 1$

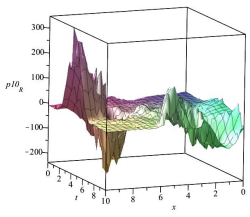

(d) Real part of p_{10} with $\sigma = 2$

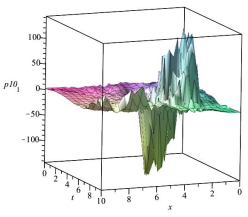

(e) Imaginary part of p_{10} with $\sigma = 2$

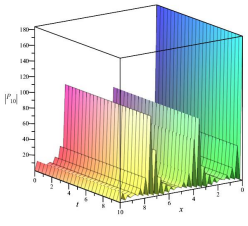

(f) Modulus of p_{10} with $\sigma = 1$

Figure 8. The solution p_{10} of Eq (1.1) with $\eta_1 = -140$, $\eta_2 = -10.5$, $\eta_3 = 10.5$, $\eta_4 = 1$, $\eta_5 = 1.5$, $\eta_6 = -17$ and $\zeta_0 = 0$.

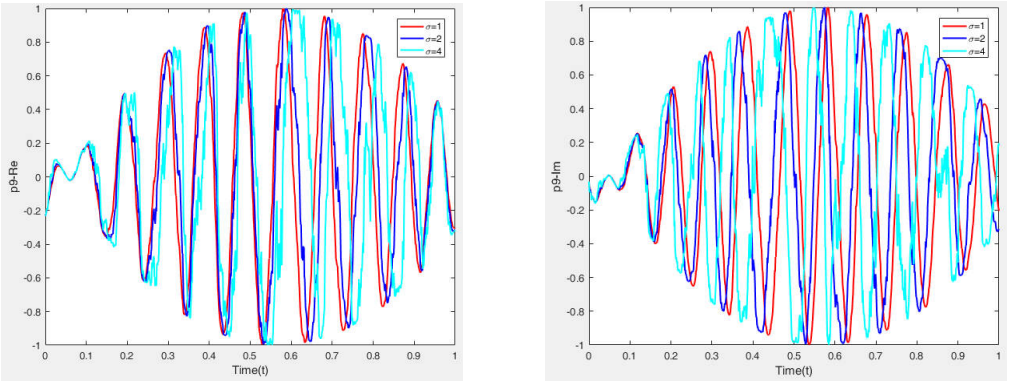

(a) Real part of p_9 (b) Imaginary part of p_9

Figure 9. The influence of random factors on solution p_9 of Eq (1.1) with $\sigma = 1$, $\sigma = 2$, and $\sigma = 6$.

6. Conclusions

This article enriches the research on the traveling wave solution of Eq (1.1), and combines visualization techniques to analyze the morphological changes and propagation characteristics of traveling wave solutions. Compared with other literature, this article provides more forms of exact solutions, such as the Jacobian elliptic functions, which is beneficial for people to have a more comprehensive understanding of the morphological changes of the exact solution of Eq (1.1). By applying random interference factors of different intensities, the influence of random factors on the solution of Eq (1.1) were explored, providing more references for further in-depth research on the internal mechanism of Eq (1.1) and its practical application. These research results are also beneficial for people to better understand the propagation characteristics of traveling waves and promote the wider application of the system Eq (1.1).

Author contributions

Da Shi: Writing-Review & Editing; Writing-Original Draft; Zhao Li: Software; Dan Chen: Formal Analysis. All authors have read and approved the final version of the manuscript for publication.

Use of AI tools declaration

The authors declare they have not used Artificial Intelligence (AI) tools in the creation of this article.

Conflict of interest

The authors declare no conflicts of interest.

References

1. A. Hasegawa, F. Tappert, Transmission of stationary nonlinear optical pulses in dispersive dielectric fibers. II. normal dispersion, *Appl. Phys. Lett.*, **23** (1973), 171–172. https://doi.org/10.1063/1.1654847
2. L. F. Mollenauer, R. H. Stolen, J. P. Gordon, Expermental observation of picosecond pulse narrowing and soliton in optical fibers, *Phys. Rev. Lett.*, **45** (1980), 1095–1098. https://doi.org/10.1103/PhysRevLett.45.1095
3. D. Krökel, N. J. Halas, G. Giuliani, D. Grischkowsky, Dark-pulse propagation in optical fibers, *Phys. Rev. Lett.*, **60** (1988), 29–32. https://doi.org/10.1103/PhysRevLett.60.29
4. A. M. Weiner, J. P. Heritage, R. J. Hawkins, R. N. Thurston, E. M. Kirschner, D. E. Leaird, et al., Experimental observation of the fundamental dark soliton in optical fibers, *Phys. Rev. Lett.*, **61** (1988), 2445–2448. https://doi.org/10.1103/PhysRevLett.61.2445
5. M. S. Ahmed, A. A. S. Zaghrout, H. M. Ahmed, Travelling wave solutions for the doubly dispersive equation using improved modified extended tanh-function method, *Alex. Eng. J.*, **61** (2022), 7987–7994. https://doi.org/10.1016/j.aej.2022.01.057
6. W. B. Rabie, H. M. Ahmed, A. Darwish, H. H. Hussein, Construction of new solitons and other wave solutions for a concatenation model using modified extended tanh-function method, *Alex. Eng. J.*, **74** (2023), 445–451. https://doi.org/10.1016/j.aej.2023.05.046
7. D. Shi, Z. Li, New optical soliton solutions to the (n+1) dimensional time fractional order Sinh-Gordon equation, *Results Phys.*, **51** (2023), 106669. https://doi.org/10.1016/j.rinp.2023.106669
8. T. A. Khalil, N. Badra, H. M. Ahmed, W. B. Rabie, Optical solitons and other solutions for coupled system of nonlinear Biswas-Milovic equation with Kudryashov's law of refractive index by Jacobi elliptic function expansion method, *Optik*, **253** (2022), 168540. https://doi.org/10.1016/j.ijleo.2021.168540
9. D. C. Lu, A. R. Seadawy, M. Arshad, Solitary wave and elliptic function solutions of sinh-Gordon equation and its applications, *Mod. Phys. Lett. B*, **33** (2019), 1950436. https://doi.org/10.1142/S0217984919504360
10. H. Triki, A. M. Wazwaz, Sub-ODE method and soliton solutions for the variable-coefficient mKdV equation, *Appl. Math. Comput.*, **214** (2009), 370–373. https://doi.org/10.1016/j.amc.2009.04.003
11. G. W. Wang, K. T. Yang, H. C. Gu, F. Guan, A. H. Kara, A (2+1)-dimensional sine-Gordon and sinh-Gordon equations with symmetries and kink wave solutions, *Nucl. Phys. B*, **953** (2020), 114956. https://doi.org/10.1016/j.nuclphysb.2020.114956
12. H. H. Sheng, G. F. Yu, Rational solutions of a (2+1)-dimensional sinh-Gordon equation, *Appl. Math. Lett.*, **101** (2020), 106051. https://doi.org/10.1016/j.aml.2019.106051
13. N. A. Kudryashov, Painlevé analysis and exact solutions of the Korteweg-de Vries equation with a source, *Appl. Math. Lett.*, **41** (2015), 41–45. https://doi.org/10.1016/j.aml.2014.10.015
14. G. Q. Xu, Y. P. Liu, W. Y. Cui, Painlevé analysis, integrability property and multiwave interaction solutions for a new (4+1)-dimensional KdV-Calogero-Bogoyavlenkskii-Schiff equation, *Appl. Math. Lett.*, **132** (2022), 108184. https://doi.org/10.1016/j.aml.2022.108184

15. T. Y. Zhou, B. Tian, Auto-Bäcklund transformations, Lax pair, bilinear forms and bright solitons for an extended (3+1)-dimensional nonlinear Schrödinger equation in an optical fiber, *Appl. Math. Lett.*, **133** (2022), 108280. https://doi.org/10.1016/j.aml.2022.108280

16. D. Y. Yang, B. Tian, H. Y. Tian, C. C. Wei, W. R. Shan, Y. Jiang, Darboux transformation, localized waves and conservation laws for an M-coupled variable-coefficient nonlinear Schrödinger system in an inhomogeneous optical fiber, *Chaos Soliton. Fract.*, **156** (2022), 111719. https://doi.org/10.1016/j.chaos.2021.111719

17. Y. Chen, Q. Wang, B. Li, The stochastic soliton-like solutions of stochastic KdV equations, *Chaos Soliton. Fract.*, **23** (2005), 1465–1473. https://doi.org/10.1016/j.chaos.2004.06.049

18. S. S. Ray, S. Singh, New exact solutions for the wick-type stochastic Kudryashov-Sinelshchikov equation, *Commun. Theor. Phys.*, **67** (2017), 197–206. https://doi.org/10.1088/0253-6102/67/2/197

19. A. H. Arnous, A. M. Elsherbeny, A. Secer, M. Ozisik, M. Bayram, N. A. Shah, et al., Optical solitons for the dispersive concatenation model with spatio-temporal dispersion having multiplicative white noise, *Results Phys.*, **56** (2024), 107299. https://doi.org/10.1016/j.rinp.2023.107299

20. K. Itô, Stochastic integral, *Proc. Imp. Acad.*, **20** (1944), 519–524. https://doi.org/10.3792/pia/1195572786

21. F. F. Liu, X. Lü, J. P. Wang, Dynamical behavior and modulation instability of optical solitons with spatio-temporal dispersion, *Phys. Lett. A*, **496** (2024), 129317. https://doi.org/10.1016/j.physleta.2024.129317

22. E. M. E. Zayed, A. H. Arnous, A. Secer, M. Ozisik, M. Bayram, N. A. Shah, et al., Highly dispersive optical solitons in fiber Bragg gratings for stochastic Lakshmanan-Porsezian-Daniel equation with spatio-temporal dispersion and multiplicative white noise, *Results Phys.*, **55** (2023), 107177. https://doi.org/10.1016/j.rinp.2023.107177

23. T. Y. Han, Y. Y. Jiang, J. J. Lyu, Chaotic behavior and optical soliton for the concatenated model arising in optical communication, *Results Phys.*, **58** (2024), 107467. https://doi.org/10.1016/j.rinp.2024.107467

24. W. W. Mohammed, C. Cesarano, D. Rizk, E. S. Aly, M. El-Morshedy, Impact of white noise on the exact solutions of the stochastic Riemann wave equation in quantum mechanics, *Symmetry*, **15** (2023), 2070. https://doi.org/10.3390/sym15112070

25. C. S. Liu, Trial equation method and its applications to nonlinear evolution equations, *Acta Phys. Sin.*, **54** (2005), 2505–2509. https://doi.org/10.7498/aps.54.2505

26. Y. Kai, Y. X. Li, A study of Kudryashov equation and its chaotic behaviors, *Wave. Random Complex*, 2023, 1–17. https://doi.org/10.1080/17455030.2023.2172231

27. Y. Kai, L. K. Huang, Dynamic properties, Gaussian soliton and chaotic behaviors of general Degasperis-Procesi model, *Nonlinear Dyn.*, **111** (2023), 8687–8700. https://doi.org/10.1007/s11071-023-08290-4

28. J. Wang, Z. Li, A dynamical analysis and new traveling wave solution of the fractional coupled Konopelchenko-Dubrovsky model, *Fractal Fract.*, **8** (2024), 341. https://doi.org/10.3390/fractalfract8060341

29. C. Y. Liu, The chaotic behavior and traveling wave solutions of the conformable extended Korteweg-de-Vries model, *Open Phys.*, **22** (2024), 20240069. https://doi.org/10.1515/phys-2024-0069

30. C. S. Liu, Travelling wave solutions to 1+1 dimensional dispersive long wave equation, *Chinese Phys.*, **14** (2005), 1710–1715. https://doi.org/10.1088/1009-1963/14/9/005

AIMS Press